Draft version February 13, 2012
Preprint typeset using LaTeX style emulateapj v. 5/2/11

arXiv:1202.2150v1 [astro-ph.CO] 9 Feb 2012

THE Y_{SZ}–Y_X SCALING RELATION AS DETERMINED FROM *PLANCK* AND *CHANDRA*

Eduardo Rozo[1,2], Alexey Vikhlinin[3,4], Surhud More[1]

Draft version February 13, 2012

ABSTRACT

SZ clusters surveys like *Planck*, the South Pole Telescope, and the Atacama Cosmology Telescope, will soon be publishing several hundred SZ-selected systems. The key ingredient required to transport the mass calibration from current X-ray selected cluster samples to these SZ systems is the Y_{SZ}–Y_X scaling relation. We constrain the amplitude, slope, and scatter of the Y_{SZ}–Y_X scaling relation using SZ data from *Planck* and X-ray data from *Chandra*. We find a best fit amplitude of $\ln(D_A^2 Y_{SZ}/CY_X) = -0.202 \pm 0.024$ at the pivot point $CY_X = 8 \times 10^{-5}$ Mpc^2. This corresponds to a Y_{SZ}/Y_X-ratio of 0.82 ± 0.024, in good agreement with X-ray expectations after including the effects of gas clumping. The slope of the relation is $\alpha = 0.916 \pm 0.032$, consistent with unity at $\approx 2.3\sigma$. We are unable to detect intrinsic scatter, and find no evidence that the scaling relation depends on cluster dynamical state.

Subject headings: clusters

1. INTRODUCTION

The Sunyaev–Zeldovich effect — i.e. the prediction that the hot intra-cluster gas of massive galaxy clusters will scatter CMB photons to produce a unique frequency signature — traces back to 1972 (Sunyaev & Zeldovich 1972). Despite early detections of this effect (Gull & Northover 1976), it is only recently that instrumentation advances have made large scale SZ searches feasible. There are three such ongoing surveys: one carried out with the South Pole Telescope (SPT Carlstrom et al. 2011), one with the Atacama Cosmology Telescope (ACT Fowler et al. 2007), and one using the *Planck* satellite (Planck Collaboration 2011e). All three surveys have published initial cluster samples (Vanderlinde et al. 2010; Marriage et al. 2011; Planck Collaboration 2011d), and are expected to eventually publish hundreds of SZ selected systems out to $z = 1$ and beyond. If the scaling relation between the integrated SZ signal and cluster mass can be adequately calibrated, then these cluster samples may be used to constrain the growth of large scale structure in the universe, which can in turn provide critical constraints on dark energy models (e.g. Holder et al. 2001). Indeed, both SPT and ACT have already derived cosmological constraints from their current samples (Vanderlinde et al. 2010; Sehgal et al. 2011; Benson et al. 2011).

Unfortunately, at this time no single method provides masses of individual clusters with a required $\sim 5\%$ uncertainty. X-ray hydrostatic measurements are observationally expensive and limited to a subset of relaxed systems. Numerical simulations suggest that hydrostatic mass estimates can be biased low anywhere between 10% to 30% (Nagai et al. 2007; Piffaretti & Valdarnini 2008; Jeltema et al. 2008; Lau et al. 2009; Meneghetti et al. 2010; Rasia et al. 2012). Weak lensing estimates are in principle unbiased, but specific implementations can result in $\approx 5\% - 10\%$ biases depending on the fitting procedure (typically biased high when using NFW fitting formulae Becker & Kravtsov 2010; Meneghetti et al. 2010; Rasia et al. 2012), and exhibit large intrinsic scatter. In addition, without the help from X-ray data, the derived SZ signal from the current generation surveys has a comparatively large scatter at a fixed mass (Benson et al. 2011; Planck Collaboration 2011d). Mass calibration using velocity dispersions is also possible (e.g. Evrard et al. 2008; Sifon et al. 2012), but subject to velocity bias. Therefore, the precise calibration of the cluster masses from SZ surveys will be possible only through a combined analysis of the SZ, X-ray, and optical data. Consequently, all three of the on-going SZ experiments are devoting significant effort for extensive X-ray and weak lensing follow-up of the SZ-selected systems (Andersson et al. 2010; Foley et al. 2011; Planck Collaboration 2011b,f; Menanteau et al. 2011).

Another possibility, however, is simply to transfer the existing calibration of the mass-proxy relations in the X-ray samples (e.g. Arnaud et al. 2007; Allen et al. 2008; Vikhlinin et al. 2009; Arnaud et al. 2010; Mantz et al. 2010) using the correlation of the cluster SZ parameters with the X-ray proxies (e.g. Benson et al. 2011). An important step in this process is to verify a tight correlation between the integrated SZ signal, Y_{SZ}, and its X-ray analog, $Y_X = T_X \times M_{\mathrm{gas},X}$ (Kravtsov et al. 2006, see section 1.1 for more precise definitions of Y_{SZ} and Y_X). In addition to transferring the mass calibration, the $Y_{SZ} - Y_X$ relation can be used to verify some key predictions of the structure formation theory which is used for applying the cosmological models to the cluster data. First, numerical simulations consistently show that both Y_{SZ} and Y_X have low scatter at a fixed mass ($\approx 10\% - 15\%$, Nagai 2006; Kravtsov et al. 2006; Stanek et al. 2010; Fabjan et al. 2011; Kay et al. 2011). Thus, we can expect the Y_{SZ}–Y_X relation to have very low scatter, especially since these parameters approxi-

[1] Kavli Institute for Cosmological Physics, Chicago, IL 60637, USA
[2] Department of Astronomy, University of Chicago, Chicago, IL 60637, USA
[3] Space Research Institute (IKI), Profsoyuznaya 84/32, Moscow 117810, Russia
[4] Harvard-Smithsonian Center for Astrophysics, 60 Garden St., Cambridge, MA 02138, USA

mate the same physical quantity, the thermal energy in the cluster gas. Second, these same simulations predict nearly self-similar evolution in the $Y - M$ relation for both Y_X and Y_{SZ}, so we expect the Y_{SZ}–Y_X relation to have nearly the same normalization at both low and high redshifts.

The Y_{SZ}–Y_X relation has been reported in several recent works — by Andersson et al. (2010) at high-z using SPT and *Chandra*, and at low-z by Planck Collaboration (2011a) using Planck and *XMM-Newton*. The results are generally in line with the theoretical expectations — Y_{SZ} follows Y_X with a small overall offset. However, there are several issues which warrant further study. The overall offset between Y_X and Y_{SZ} is expected because real clusters are non-isothermal and slightly non-uniform. Given the overall ρ^2 weighting of X-ray emission versus the ρ weighting of the SZ-signal, one naturally expects the two quantities to differ (see below for further details). Based on the analysis of *XMM-Newton* temperature profiles in a "representative" sample of clusters, Arnaud et al. (2010) predicted $Y_{SZ}/Y_X = 0.924$. The mean offset in the SPT/*Chandra* sample of Andersson et al. (2010) is somewhat below this prediction, $Y_{SZ}/Y_X = 0.82 \pm 0.07$. The mean offset in the Planck/*XMM-Newton* sample is $1\,\sigma$ above, $Y_{SZ}/Y_X = 0.95 \pm 0.03$ (Planck Collaboration 2011a). While the difference in the Y_{SZ}/Y_X ratio is relatively large, it is not significant because of the large errors in the Andersson et al. (2010) measurement, so additional measurements that reduce the statistical uncertainty of *Chandra* estimates of the Y_{SZ}/Y_X ratio are of great interest. This is particularly true in light of known differences in instrument calibration between *Chandra* and *XMM* so having a low-redshift calibration of this ratio using *Chandra* is of significant interest. Finally, the scatter in the *Planck*/*XMM* Y_{SZ}–Y_X relation is 23% ± 2%, which is significantly larger than the expected ≈ 10% scatter, so confirmation of this observation is important.

The goal of this paper is to measure the local $Y_{SZ} - Y_X$ relation independently using overlapping clusters in the Planck and Vikhlinin et al. (2009) *Chandra* sample. This is the first step towards *Chandra*-based calibration of the local $Y_{SZ} - M$ relation. We defer the actual calibration of the Y_{SZ}–M relation to an upcoming paper, where we simultaneously consider several the Y_{SZ}–M scaling relation as calibrated by several groups (Rozo et al. 2011). In this context, we emphasize that the Chandra X-ray results quoted here are derived from the gas temperature and gas density models for individual clusters taken from Vikhlinin et al. (2009). Consequently, this work and that of Vikhlinin et al. (2009) are fully self-consistent in all definitions.

Throughout this work, we assume a flat ΛCDM cosmology with $\Omega_m = 0.3$ and $h = 0.72$. This convention matches that of Vikhlinin et al. (2009).

1.1. *What We Mean by the Y_{SZ}/Y_X Ratio*

The Y_{SZ} signal of a galaxy cluster is related to the total pressure of the intra-cluster gas within the cluster's volume via

$$D_A^2 Y_{SZ} = C \int dV \rho_{gas}(\mathbf{x}) T(\mathbf{x}) \qquad (1)$$

where D_A is the angular diameter distance, and C is a constant that switches the units back and forth from $M_\odot$keV to Mpc^2. The constant C is given by

$$C = \frac{\sigma_T}{m_e c^2} \frac{1}{\rho_{\rm gas}/n_e} = 1.406 \times \frac{10^{-5}\ \rm Mpc^2}{10^{14}\ {\rm keV} M_\odot}, \qquad (2)$$

where σ_T is the Thompson cross-section, and $\rho_{\rm gas}/n_e = 1.149\, m_p$ for fully ionized plasma with the cosmic He abundance and abundance of heavier elements set at solar. Arnaud et al. (2010) assume a heavy-element abundance that is 0.3 solar, which differs from the above value by less than 1%, a difference that is completely negligible for our purposes.

From equation 1, it is apparent that the combination $D_A^2 Y_{SZ}$ will scale with CY_X where $Y_X = M_{gas} \times T_X$ (see section 3.3 for our precise definition of M_{gas} and T_X). Thus, we expect that the Y_{SZ}/Y_X ratio is a dimensionless number that is close to unity. Throughout this work, we will often speak about the Y_{SZ}/Y_X ratio in this fashion. In practice, however, Y_{SZ} and Y_X are cluster observables that are related via a probability distribution $P(Y_{SZ}|Y_X)$. Here, we assume $P(Y_{SZ}|Y_X)$ is a log-normal distribution, which takes the form

$$\left\langle \ln\left(D_A^2 Y_{SZ}\right) | Y_X \right\rangle = a + \alpha \ln CY_X. \qquad (3)$$

When we speak of "the Y_{SZ}/Y_X ratio", we mean the quantity $\left\langle \ln\left(D_A^2 Y_{SZ}\right) | Y_X \right\rangle - \ln CY_X$ evaluated at the pivot point of the sample. Note that if we select units such that $CY_X = 1$ at the pivot point, then the Y_{SZ}/Y_X ratio is just the amplitude a. We will work primarily in units of $CY_X = 8 \times 10^{-5}$ Mpc^2, corresponding to the pivot point for the *Chandra–Planck* cluster sample (see section 3). For brevity, we will often simply write $\ln(Y_{SZ}/Y_X)$ — as opposed to the full $\left\langle \ln D_A^2 Y_{SZ} | Y_X \right\rangle - \ln CY_X$ expression — to denote the Y_{SZ}/Y_X ratio.

2. X-RAY PREDICTIONS

Equation 1 allows one to compute the Y_{SZ} signal of a galaxy cluster based on the gas and temperature profiles of galaxy clusters. With sufficiently high quality X-ray data, both of these profiles can be observationally constrained, allowing one to directly predict the Y_{SZ} signal of a galaxy cluster from the X-ray data. Using this method, Arnaud et al. (2010) predicted that $D_A^2 Y_{SZ}/CY_X = 0.924$ or $\ln(Y_{SZ}/Y_X) = -0.08$ when T_X is defined within a $[0.15, 0.75]R_{500}$ aperture. Using the Vikhlinin et al. (2006) *Chandra* results for local relaxed clusters, we predict nearly the same ratio. Specifically, the mass-weighted temperature

$$T_{mw} = \frac{\int dV\ \rho_{gas}(\mathbf{x}) T(\mathbf{x})}{\int dV\ \rho_{gas}(\mathbf{x})}, \qquad (4)$$

is related to the spectroscopic temperature T_X via $T_{mw}/T_X = 0.928$, where T_X is measured in the $[0.15 - 1]\, R_{500}$ aperture. Using the definition for T_{mw}, we see that we can rewrite equation 1 via

$$D_A^2 Y_{SZ} = C M_{gas} T_{mw}, \qquad (5)$$

from which we find $\ln(Y_{SZ}/Y_X) = -0.07$.

It is potentially a concern that the Arnaud et al. (2010) work is based on a representative cluster sample of X-ray luminous clusters while Vikhlinin et al. (2006) include only relaxed, cool core clusters. However, empirically, there is very little difference in Y_{SZ}/Y_X for relaxed and unrelaxed clusters judging either from the X-ray predictions (Fig.9 in Arnaud et al. 2010) or the actual measurements (see Fig.4 in Planck Collaboration 2011a, and our results below). Another point of concern is slightly different apertures for T_X used in the *XMM* and *Chandra* samples. One expects that mean (emission-weighted) temperatures in the $[0.15-1]\,R_{500}$ and $[0.15-0.75]\,R_{500}$ annuli should be close because only a small fraction of the total X-ray flux comes from outside $0.75\,R_{500}$. Indeed, the $T_X([0.15, 0.75]R500)/T_X([0.15, 1]R500)$ ratios in the Chandra sample of Vikhlinin et al. (2009) are within ±0.015 of a mean value of 0.985. An analysis of the deeper pointings among the ESZ-XMM sample (G.Pratt, private comm.) shows a similar value, even though the temperature ratio for the REXCESS sample (Pratt et al. 2009) was somewhat lower on average (≈ 0.95), and showed a larger spread $0.85-1$. We proceed accordingly, and ignore the difference in the definition of TX between the two works. With this caveat in mind, we conclude that both *XMM* and *Chandra* predict $\ln(Y_{SZ}/Y_X) \simeq -0.075$ because of non-isothermal cluster temperature profiles.

There is, however, an additional complication that modifies these expectations. Specifically, when one estimates M_{gas} from X-ray data, one uses the fact that the surface brightness $S \propto \rho_{gas}^2$ to estimate $\langle\rho_{gas}^2\rangle$, averaged in radial annuli. For a uniform, spherically symmetric distribution $\langle\rho_{gas}^2\rangle = \langle\rho_{gas}\rangle^2$, so one can recover the gas density profile. In practice, however, one will typically have $\langle\rho_{gas}^2\rangle > \langle\rho_{gas}\rangle^2$. The clumping factor Q^2 is defined via

$$Q^2 = \frac{\langle\rho_{gas}^2\rangle}{\langle\rho_{gas}\rangle^2}, \tag{6}$$

so that $M_{gas}^{obs} = QM_{gas}^{true}$. By definition, $Y_X = M_{gas}^{obs}T_X$, so the Y_{SZ} to Y_X ratio takes the form

$$\frac{D_A^2 Y_{SZ}}{CY_X} = \frac{1}{Q}\frac{T_{mw}}{T_X}. \tag{7}$$

In practice, the clumping factor Q depends on radius, and the factor $1/Q$ characterizes the mean clumping correction over the radius R_{500}. Based on this discussion, we modify our X-ray expectation by a factor of Q^{-1}. If there is no substructure masking in the X-ray analysis, Q can be very large (e.g. $Q = 1.16$, Mathiesen et al. 1999), though analysis of numerical simulations that include substructure masking achieve significantly lower values of Q. Based on the analysis of Nagai et al. (2007), we set $Q = 1.05 \pm 0.05$, where the error is set to the size of the correction to account for systematic uncertainties in the simulation physics. The corresponding expectation for the Y_{SZ}/Y_X ratio is $\ln(D_A^2 Y_{SZ}/CY_X) = -0.125 \pm 0.05$.

Finally, we note that T_X measured in the X-ray can be subject to a systematic uncertainty, related to, e.g., absolute calibration of the X-ray telescope effective area. Assuming for simplicity that this results in a uniform bias of observed temperatures, $T_X^{(\mathrm{meas})} = A\,T_X^{(\mathrm{true})}$, the measured ratio of the Y's can be factorized as

$$\frac{D_A^2 Y_{SZ}}{CY_X} = \frac{1}{A\,Q}\frac{T_{mw}}{T_X}. \tag{8}$$

Discussion of the calibration-related uncertainties in T_X is beyond the scope of this paper and we proceed assuming $A = 1$. However, it is important to keep in mind a possibility of a few percent systematic error in the X-ray temperature measurements with the current calibration of the *XMM-Newton* and *Chandra* instruments. To give a handle of possible deviations of A from unity, we note that within the sample we consider in this work, the average ratio of *XMM* and *Chandra*-measured temperatures for the same cluster is $\ln(T_{XMM}/T_{Chandra}) = -0.08$ (for a detailed comparison of *XMM* and *Chandra* data on a cluster-by-cluster basis see Rozo et al. 2012, in preparation).[5]

3. DATA

3.1. *Cluster Sample*

The cluster sample employed in this work is a subset of the Early SZ (ESZ) sample published in Planck Collaboration (2011d). The ESZ sample is comprised of 189 cluster candidates identified in a blind, multi-frequency search of the all-sky maps obtained from the first ten months of observations of the *Planck* mission (Planck Collaboration 2011e). The threshold for cluster detection was set at a signal-to-noise $(S/N) \geq 6$. This ESZ sample was searched for archival *XMM* data, and a sub-sample of 88 galaxy clusters with *XMM* data were identified. Of these, 62 clusters were processed in time for publication, as detailed in Planck Collaboration (2011a). Starting from this sub-sample of 62 galaxy clusters, we identified 28 clusters with *Chandra* data that had already been analyzed using the data reduction pipeline of Vikhlinin et al. (2009). The analysis presented here is based on this sub-sample of 28 galaxy clusters, which is summarized in Table 1. 20 of these are relaxed galaxy clusters, and 8 are merging systems. A plot of the Y_{SZ} vs Y_X data for the galaxy clusters is shown in Figure 1.

3.2. *Planck Data*

For each of our galaxy clusters, (Planck Collaboration 2011a) estimated the integrated Compton parameter Y_{SZ} using a matched-filter algorithm. The matched filter assumes an Arnaud et al. (2010) pressure profile, which is used to predict the CMB temperature perturbation $\delta T(\theta)$ of each galaxy cluster in each of the *Planck* frequency bands. In order to perform the fit, the clusters are first assigned a putative R_{500} radius based on the *XMM* X-ray data and the M–Y_X scaling relation of Arnaud et al. (2010). The amplitude of the matched-filter, which can be expressed in terms of the integrated Compton parameter Y_{SZ}, is then fit using the temperature data within a projected aperture of $5R_{500}$. We note that the shape of the matched filter is held fixed in the Planck Collaboration (2011a) analysis, but their systematics tests demonstrate that varying the shape of the filter within tolerable levels does not significantly impact

---

[5] The quoted ratio does *not* correct for the difference between the temperature definitions used in the relevant *XMM* and *Chandra* works as noted earlier.

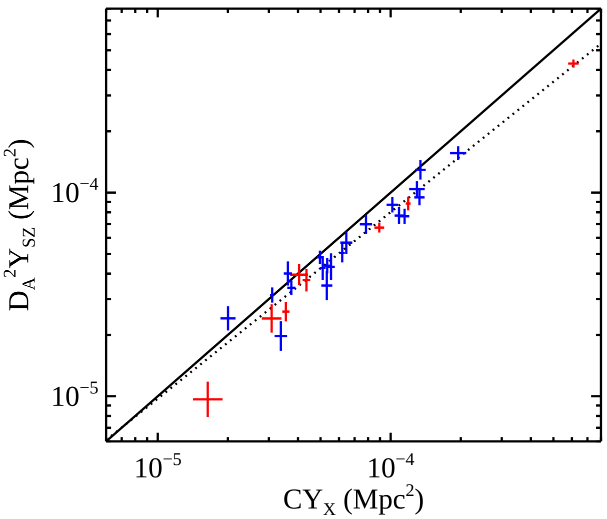

FIG. 1.— The relation between the Planck $D_A^2Y_{SZ}$ and *Chandra* CY_X measured in the same aperture, R_{500} provided by *XMM*-Newton mass estimates. Blue and red crosses represent dynamical relaxed and merging clusters, respectively (per the Vikhlinin et al. (2009) classification). The solid line shows a 1-1 relation, while the dotted line is our best fit relation. The amplitude at the pivot point corresponds to $D_A^2Y_{SZ}/CY_X = 0.82$.

the recovered scaling relations. The median error in the recovered Y_{SZ} values for our cluster sample is 11%, and systematic uncertainties due to instrumental beam size and radio point source contamination are all expected be at the few percent level at most. Note that because Planck Collaboration (2011a) assumed $h = 0.7$ while we assume $h = 0.72$, we must rescale the $D_A^2Y_{SZ}$ values in Planck Collaboration (2011a) appropriately. Further, the Planck team uses the redshifts listed for the clusters in the NED and SIMBAD databases while we use the redshifts of the dominant central galaxies. We believe the latter approach is more robust because it allows one to avoid contamination by projection effects in some cases. Therefore, we rescaled all angular diameter distances to our adopted z values. The cluster redshifts, along with the rescaled Y_{SZ} values, are detailed in Table 1.

3.3. *Chandra Data*

Our analysis is based on the sub-sample of ESZ galaxy clusters from Planck Collaboration (2011d) that have *Chandra* data that was reduced as part of the work in Vikhlinin et al. (2009), described in full detail in Vikhlinin et al. (2005, 2006). Here, we provide only a brief summary. We note that not all galaxy clusters in our analysis are included in the Vikhlinin et al. (2009) sample. These are the clusters which were analyzed by Vikhlinin et al. (2009) but not included in the flux-limited sample used in their cosmological analysis. The full list of clusters employed in our analysis is presented in Table 1.

We use the available *Chandra* data to estimate $Y_X = M_{gas} \times T_X$ for each of the clusters in our sample, where M_{gas} is the total gas mass within the radius R_{500} employed by Planck Collaboration (2011a), and T_X is the spectroscopic temperature within an annulus $R \in [015, 1]R_{500}$. To estimate M_{gas}, we rely on analytic fits to the gas density profiles of individual clusters. The fits were based on the X-ray brightness profiles in the 0.7–2 keV energy band measured with *Chandra* and *ROSAT* PSPC (see Vikhlinin et al. (2009) for details). All detectable X-ray substructures were masked out from the profile measurements to minimize the impact of gas clumping. The X-ray flux in the $0.7 - 2$ keV band is very insensitive to the plasma temperature so long as $T \gtrsim 2$ keV, as in the case of the sample under consideration. Nevertheless, we apply the appropriate temperature and metallicity corrections to the X-ray profile to estimate M_{gas}. The mean cluster temperature reported by Vikhlinin et al. (2009) corresponds to the single-temperature fit to the X-ray spectrum in the $0.6 - 10$ keV band extracted within an annulus $[0.15, 1]R_{500}$. The median error in the recovered Y_X values for our cluster sample is 3%, nearly identical to the median error in the corresponding *XMM* X-ray data in Planck Collaboration (2011a).

3.4. *On the Importance of Apertures*

As already mentioned in section 1.1, we ignore any radial dependence on the Y_{SZ}–Y_X scaling relation. In other words, we are explicitly assuming that the parameters a and α are insensitive to the radius at which both Y_{SZ} and Y_X are evaluated. This is clearly not true over arbitrarily large radial ranges, but we expect any evolution over the range of radii probed to be at the $\lesssim 1\%$ level, so long as both Y_{SZ} and Y_X are always measured within the same aperture. Since we rely on the SZ data from Planck Collaboration (2011a), we have to use the same metric apertures adopted in that work. Specifically, to estimate Y_X, we first measure M_{gas} within the assigned R_{500} aperture, and multiply this by the estimated temperature T_X as quoted in Vikhlinin et al. (2009). We do not remeasure T_X since the X-ray temperature is robust to modest changes in the assigned R_{500} radius of a cluster. A relation between *Planck*-measured Y_{SZ} and the *Chandra* Y_X values is shown in Fig. 1. There is an obvious, tight correlation that is nearly linear, with no obvious offset between merging and relaxed systems.

4. LIKELIHOOD MODEL

Because we will be assuming log-normal models throughout, we begin by defining y_x and y_{sz} via

$$y_x = \ln\left(\frac{CY_X}{8\times10^{-5}\ \mathrm{Mpc}^2}\right) \tag{9}$$

$$y_{sz} = \ln\left(\frac{D_A^2Y_{SZ}}{8\times10^{-5}\ \mathrm{Mpc}^2}\right). \tag{10}$$

We divide both Y_X and Y_{SZ} by 8×10^{-5} Mpc^2 so that both quantities are still measured in the same units, while simultaneously shifting the pivot point of the y_{sz}–y_x scaling relation to ensure the amplitude and slope of the best-fit Y_{SZ}–Y_X relation are nearly uncorrelated.

For each cluster, we assume that the observed y_x value is given by

$$y_x = \bar{y}_x + \delta_y \tag{11}$$

where $\bar{y}_x$ is the true value, and δ_y is a random gaussian fluctuation of zero mean and $\langle\delta_y^2\rangle = \sigma_x^2$, where σ_x is the assigned observational error. A similar expression holds for y_{sz} in terms of the true SZ signal $\bar{y}_{sz}$. The true values $\bar{y}_{sz}$ and $\bar{y}_x$ are themselves related via a probability distribution $P(\bar{y}_{sz}|\bar{y}_x)$ that characterizes the scaling relation. We assume this is a log-normal distribution of mean

$$\langle y_{sz}|y_x\rangle = a + \alpha y_x \tag{12}$$

and variance $\sigma^2_{sz|x}$, so that $\sigma_{sz|x}$ is the intrinsic scatter in the Y_{SZ}–Y_X relation. We assume this scaling relation is redshift independent, so a, α, and $\sigma_{sz|x}$ are all redshift independent. Note that because we have chosen our units to ensure that $y_x = 0$ at $CY_X = 8 \times 10^{-5}$ Mpc^2, the amplitude a is the Y_{SZ}/Y_X ratio at this scale.

The probability that a galaxy cluster has observed values y_x and y_{sz} can be written as

$$P(y_{sz}, y_x) = \int d\bar{y}_x d\bar{y}_{sz}\ P(y_{sz}, y_x|\bar{y}_{sz}, \bar{y}_x)P(\bar{y}_{sz}, \bar{y}_x) \tag{13}$$

$$= \int d\bar{y}_x d\bar{y}_{sz}\ P(y_{sz}|\bar{y}_{sz})P(y_x|\bar{y}_x)P(\bar{y}_{sz}|\bar{y}_x)P(\bar{y}_x), \tag{14}$$

where we are using the fact that the observational errors in y_x and y_{sz} are uncorrelated. In principle, there can be a small amount of covariance induced by aperture effects. We discuss this effect in more detail below, but the main conclusion is that the effect is negligible for our purposes, and so we will ignore this effect in our discussion.

Note the probability $P(y_{sz}, y_x)$ depends on the distribution $P(\bar{y}_x)$ of the cluster sample under consideration, which depends on cluster selection effects. We consider two possibilities, namely a flat prior for the value $\bar{y}_x$, and a power-law distribution in Y_X, corresponding to $P(\bar{y}_x) = \exp(-\beta y_x)$. The slope β can then be set to the expected slope for a WMAP7 cosmology. In practice, neither is exact, but it can help give us a sense of the level of systematic uncertainty in our data due to selection effects.

Setting $P(\bar{y}_x)$ to a constant, integration of equation 14 allows us to conclude that $P(y_{sz}, y_x)$ is a Gaussian distribution

$$P(y_{sz}, y_x) = G(\delta; \sigma^2_{tot}) \tag{15}$$

$$= \frac{1}{\sqrt{2\pi\sigma^2_{tot}}} \exp\left(-\frac{1}{2}\frac{\delta^2}{\sigma^2_{tot}}\right) \tag{16}$$

where

$$\delta = y_{sz} - (a + \alpha y_x) \tag{17}$$

$$\sigma^2_{tot} = \alpha^2\sigma^2_x + \sigma^2_{sz} + \sigma^2_{sz|x}. \tag{18}$$

For a power-law distribution $P(y_x) \propto \exp(-\beta y_x)$, we find

$$P(y_{sz}, y_x) \propto G(\delta; \sigma^2_{tot}) \times \exp\left[-\beta\left(y_x f_{sz} + \tilde{y}_x f_x\right) + \frac{1}{2}\frac{\beta^2}{\alpha^2}\sigma^2_{tot} f_x f_{sz}\right] \tag{19}$$

where $\tilde{y}_x$ is the y_x value expected from y_{sz} from naively inverting the scaling relation, i.e.

$$\tilde{y}_x = \alpha^{-1}(y_{sz} - a). \tag{20}$$

f_x and f_{sz} are the fraction of the total variance due to y_x and y_{sz} respectively,

$$f_x = \frac{\alpha^2\sigma^2_x}{\sigma^2_{tot}} \tag{21}$$

$$f_{sz} = \frac{\sigma^2_{sz} + \sigma^2_{sz|x}}{\sigma^2_{tot}}. \tag{22}$$

Note that for $\beta = 0$ (i.e. a flat prior), we recover equation 16, as we should. For our fiducial analysis, we will assume $\beta = 1.8$, as appropriate for a logarithmic slope of the cumulative halo mass function $N(M) \propto M^\gamma$ for $\gamma = 3$, and a self-similar slope $M \propto Y_X^{3/5}$. We have verified that setting $\beta = 0.0$ does not impact our result at any significant level, which suggests our results are not sensitive to the details of the cluster selection function. This is in good agreement with the more detailed treatment of selection effects of Planck Collaboration (2011a), who find that selection effects only impacts the slope of the best-fit relation, and then only at the $\Delta\alpha = 0.01$ level, a systematic that is three times smaller than the statistical uncertainty.

We assume that all galaxy clusters represent independent realizations of the probability distribution $P(y_{sz}, y_x)$, so that the likelihood of the entire data set is simply the product of the individual likelihoods. The posterior is

$$\mathcal{L}(a, \alpha, \sigma_{sz|x}|y_{sz}, y_x) \propto P_0(a, \alpha, \sigma_{sz|x}) \prod_{clusters} P(y_{sz}|y_x) \tag{23}$$

where P_0 is the prior, and the product is over all clusters. Note that while we are using $\sigma_{sz|x}$ as a model parameter in order to facilitate physical interpretation of our results, it is the variance $\sigma^2_{sz|x}$ that is more physical, so we adopt a flat prior on $\sigma^2_{sz|x}$, corresponding to

$$P_0(a, \alpha, \sigma_{sz|x}) \propto \sigma_{sz|x}. \tag{24}$$

4.1. *Aperture Correlations*

As detailed above, we have assumed that both Y_X and Y_{SZ} are estimated within the same aperture, and we have explicitly assumed that the Y_{SZ}/Y_X ratio is radius independent. This guarantees that the mean relation is always adequately sampled. However, any noise in the estimated aperture R_{500} necessarily induces correlated noise in the estimated Y_{SZ} and Y_X values for each clusters, and this covariance should in principle be included in the analysis. In practice, however, this is difficult to achieve because the Y_X aperture adopted is that of Planck Collaboration (2011a) rather than the R_{500} aperture that we would assign based on the Y_X measurements of Vikhlinin et al. (2009). This makes developing a self-consistent model that accounts for this covariance difficult. We can demonstrate, however, that we expect this effect to be negligible.

To see this, we go back to equation 11. We now let $\bar{y}_x$ be the true y_x value at the true radius R_{500}, while $\bar{y}_x(R)$ is the true y_x value at radius R. Assuming a power-law scaling

$$\bar{y}_x(R) = \bar{y}_x + \gamma_x \ln\left(\frac{R}{R_{500}}\right), \tag{25}$$

and letting the observed R_{500} radius be a power-law as a function of the observed Y_X, one has

$$\ln\left(\frac{R_{obs}}{R_{500}}\right) = \tau(y_x - \bar{y}_x) \tag{26}$$

where τ is some proportionality constant. Our modified equation 11 is

$$y_x = \bar{y}_x(R) + \delta_x, \tag{27}$$

so putting it all together, we arrive at

$$y_x = \bar{y}_x + \frac{1}{1-\gamma_x\tau}\delta_x. \tag{28}$$

The gas density profile of galaxy clusters is such that $\gamma_x = 1.2$, and for a self-similar scaling, $R \propto M^{1/3} \propto Y_X^{1/5}$, so $\tau = 0.2$. Thus, if we self-consistently estimated the radius R_{500} from Y_X, we would find that the variance in Y_X increases by $\approx 25\%$. Since the variance in Y_{SZ} is much larger than that in Y_X, this is not a source of concern.

What about the impact these fluctuations have on Y_{SZ}? A similar argument as the one above results in

$$y_{sz} = \bar{y}_{sz} + \frac{\gamma_{sz}\tau}{1-\gamma_{sz}\tau}\delta_x + \delta_{sz}. \tag{29}$$

Thus, the fluctuations in y_{sz} are now explicitly correlated with those in y_x. Note, however, that $\delta_x \ll \delta_{sz}$ because the SZ measurements are noisier, and that the δ_x fluctuations are themselves down-weighted by a factor ≈ 0.3. This is a very minor perturbation to the variance in y_{sz}, and the correlation coefficient between y_x and y_{sz} induced in this manner is very small indeed. To first order in $\gamma_{sz}\tau$ and $\gamma_x\tau$ we find

$$r \approx \gamma_{sz}\tau\frac{\sigma_x}{\sigma_{sz}} \approx 0.06. \tag{30}$$

Thus, we expect the covariance induced from a self-consistent estimate of R_{500} to be negligible in this case. This independence is further strengthened by the fact that R_{500} is not estimated from the *Chandra* data itself, so while we cannot adequately model the effects of aperture choice on the variance of our measurements, we do not expect these to impact our results at any significant level.

5. RESULTS

We evaluate the posterior on a grid in the 3-dimensional space spanned by the parameters a, α, and $\sigma_{sz|x}$, where the range of parameters is chosen to as to ensure that it does not impact our results. We use $a \in [-0.35, -0.05]$, $\alpha \in [0.8, 1.1]$, and $\sigma_{sz|x} \in [0, 0.25]$.[6]

Figure 3 shows our best fit scaling relation. The best fit amplitude (i.e. the Y_{SZ}/Y_X ratio), slope, and scatter are

$$a = -0.202 \pm 0.028 \tag{31}$$
$$\alpha = 0.916 \pm 0.035 \tag{32}$$
$$\sigma_{sz|x} = 0.082 \pm 0.035. \tag{33}$$

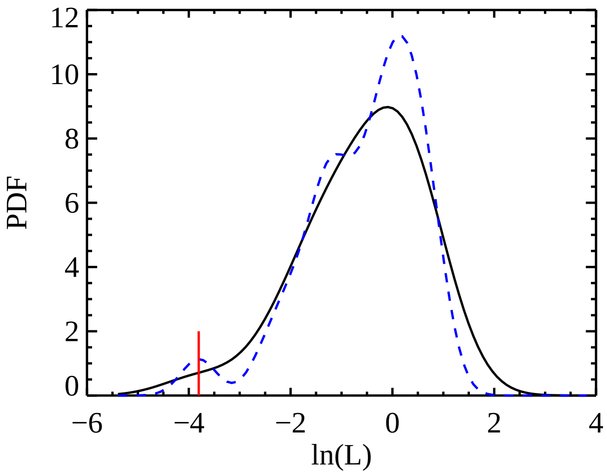

FIG. 2.— The distribution of the log-likelihood value from our cluster sample. We use our best fit model to evaluate the log-likelihood of each clusters, and a Gaussian Kernel Density Estimator (KDE) to estimate the density distribution. The black line uses Silverman's rule of thumb to set the width of the KDE (i.e. the width of the Gaussian is set to $1.34\sigma/N^{0.2}$ where N is the number of samples). The dashed blue curve halves this width, and is obviously under-smoothed. There are no glaring outliers. The most discrepant cluster is A2163 (solid red line), which has a low likelihood because of it's extremely large mass.

In all cases, the quoted values are the mean of the distribution, and the error is the standard deviation of the marginalized distribution. The slope is marginally consistent with $\alpha = 1$ ($\approx 2.3\sigma$ offset).

We have tested the sensitivity of our result to outliers by performing jackknife resamples of our galaxy clusters, and repeating our analysis. The resulting mean and standard deviation are

$$a = -0.202 \pm 0.024 \tag{34}$$
$$\alpha = 0.916 \pm 0.032 \tag{35}$$
$$\sigma_{sz|x} = 0.083 \pm 0.021 \tag{36}$$

The central values and error estimates are essentially identical to those derived from our full likelihood analysis, demonstrating that there are no large outliers. This can be furthered evidence by evaluating the log-likelihood of each individual cluster. The distribution of log-likelihoods is shown in Figure 2. The least likely cluster is A2163, reflecting the extremely large mass of this system. By the same token, A2163 significantly increases the lever-arm with which the slope of the Y_{SZ}–Y_X relation can be constrained, and has an important impact on the fit. Removing A2163 from the fit results in a slope $\alpha = 0.906 \pm 0.046$. The error increases significantly, but the deviation of α from unity is still 2σ.

We test whether the scatter of the Y_{SZ}–Y_X relation is consistent with zero or not by focusing not on the scatter, but on the variance, $\sigma^2_{sz|x}$, which is the more physical parameter. The marginalized likelihood for the variance $\sigma^2_{sz|x}$ is shown in Figure 4. We see that the data is consistent with zero variance. We can place an upper limit on the variance, $\sigma^2_{sz|x} \leq 0.021$ (95% CL), corresponding to $\sigma_{sz|x} \leq 0.144$.

We also explicitly consider the Y_{SZ}–Y_X relation with

---

[6] In section 6, we repeat our analysis using data published in Planck Collaboration (2011a). When doing so, we always make sure the extent of our multidimensional grid completely covers the high-likelihood regions in parameters space.

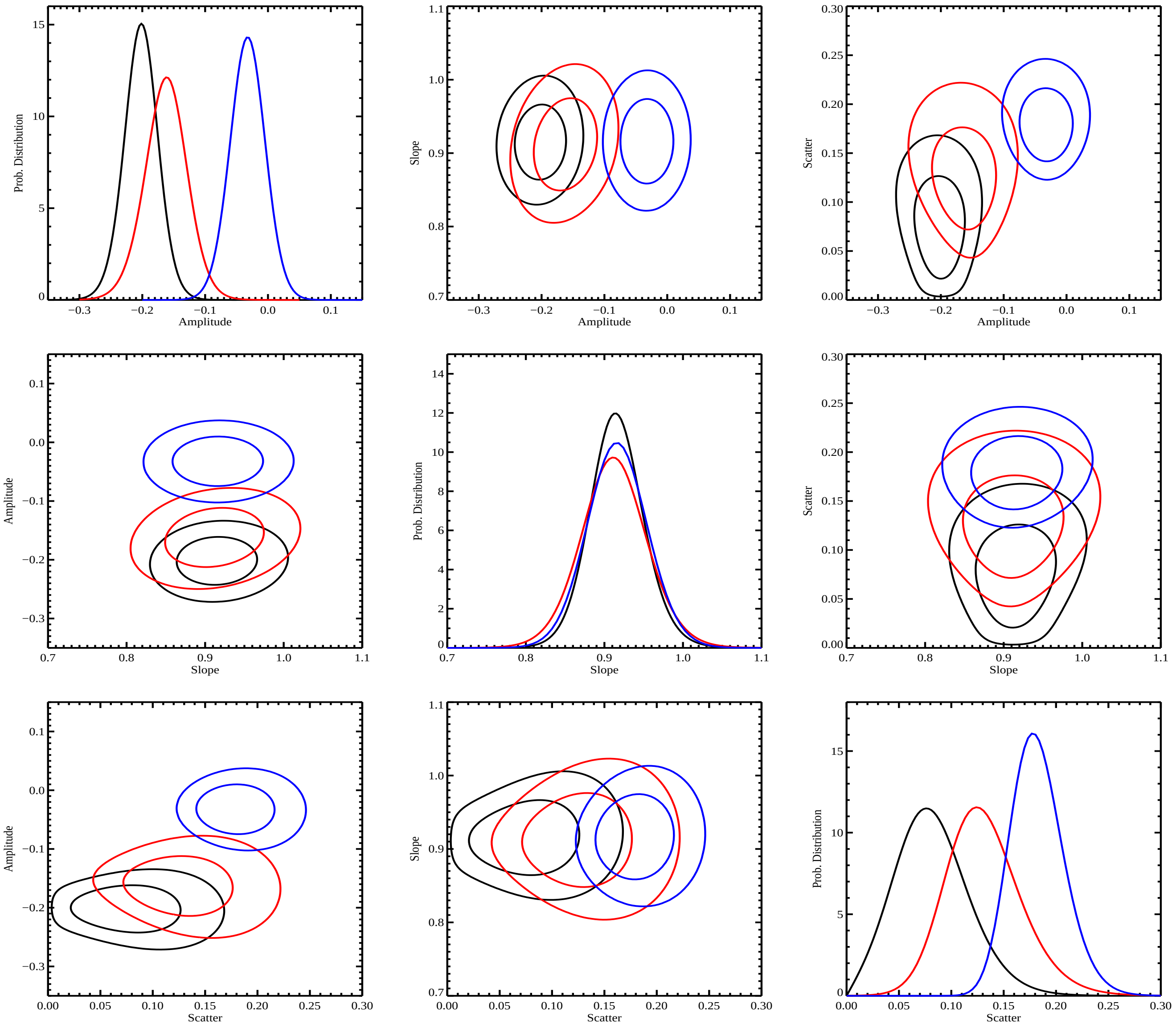

FIG. 3.— Best-fit parameters for the Y_{SZ}–Y_X scaling relation. Black curves are obtained using *Chandra* data and the cluster sample in Table 1. Red and blue curves are using the Planck Collaboration (2011a) data. The red curves show the results when we restrict our analysis of the Planck Collaboration (2011a) data to the same galaxy clusters that constitute our *Chandra* sample. The blue curves include all galaxy clusters in Planck Collaboration (2011a). All confidence regions are 68% and 95% likelihood contours respectively.

a fixed slope of unity ($\alpha = 1$). The scatter is somewhat increased to $\sigma_{sz|x} = 0.120 \pm 0.033$. The uncertainty in the amplitude also increases, reflecting the additional intrinsic scatter required to fit all the data. We find $a = -0.201 \pm 0.032$. In this context, we also investigate whether the resulting amplitude is sensitive to the dynamical state of the galaxy clusters. We split the clusters depending on whether they are relaxed or unrelaxed, using the same criteria employed in Vikhlinin et al. (2009). The best fit amplitude for the relaxed and unrelaxed cases is $a = -0.17 \pm 0.04$ and $a = -0.26 \pm 0.06$, consistent with no systematic offset between the two.

6. DISCUSSION

6.1. *Comparison to Previous Work*

We compare our best fit Y_{SZ}–Y_X scaling relation to other empirical investigations of the Y_{SZ}/Y_X ratio. There are several analysis of the SZ and X-ray properties of galaxy clusters, but most cannot be straight forwardly compare to ours. Bonamente et al. (2008) do not explicitly consider the Y_{SZ}–Y_X relation, but simply note that an isothermal model with no gas clumping gives a good fit to their data. This model corresponds to $\ln(Y_{SZ}/Y_X) = 0$, which is in strong conflict with our results. We note, however, that they used significantly smaller apertures (R_{2500}), and that their SZ and X-ray estimators are explicitly linked in the analysis: the SZ data helps constrain the X-ray data model and vice-versa, and the isothermal β model effectively acts as a prior relating the two data sets. Thus, it is difficult to fairly compare their analysis to ours.

On a similar vein, Comis et al. (2011) used the ACCEPT cluster catalog (Cavagnolo et al. 2009) to probe the Y_{SZ}–Y_X relation, but within an overdensity $\Delta =$

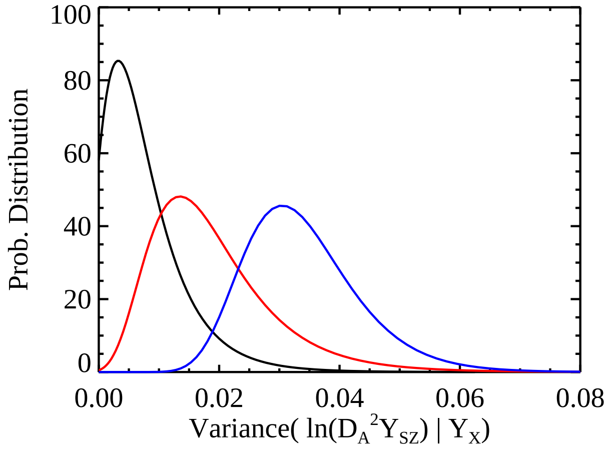

FIG. 4.— Likelihood distribution for the intrinsic variance in $\ln Y_{SZ}$ at fixed Y_X. Black, red, and blue curves are for the *Chandra–Planck* data, the *XMM–Planck* data restricted to the subset of clusters with *Chandra* data, and the full *XMM–Planck* data set.

2500. In addition, Comis et al. (2011) do not exclude the core when estimating T_X, which is expected to introduce scatter, and to systematically bias the Y_X measurements relative to what would be measured using core-excluded temperatures. Indeed, Comis et al. (2011) find both higher scatter and a higher Y_{SZ}/Y_X ratio, as we would expect. A more quantitative comparison with our results, however, is difficult.

The Planck Collaboration (2011a) analysis is the one that is closest in spirit to ours. Further, our analysis relies on their SZ-data. Switching the best fit amplitude reported in that work to the pivot point adopted here, their best fit scaling relation corresponds to $a = -0.037 \pm 0.023$ and $\alpha = 0.96 \pm 0.04$. This amplitude is significantly higher than ours at more than 4.5σ. Their slope is steeper, but consistent with ours. There is also tension between the recovered scatter of their analysis and ours, with the $\sigma_{sz|x} = 0.228$ value reported by Planck Collaboration (2011a) being ruled out by our data at very high significance.[7]

What drives the difference between our results and those of Planck Collaboration (2011a)? Two obvious possibilities that we can readily explore are the fitting method used to recover the scaling relation, and the fact that we use a subsample (28 out of 62) of the galaxy clusters employed in the Planck Collaboration (2011a) analysis.

We test the importance of the fitting method by refitting the Planck Collaboration (2011a) data with our likelihood method. We find $a = -0.032 \pm 0.028$, $\alpha = 0.917 \pm 0.039$, and $\sigma_{sz|x} = 0.182 \pm 0.025$. For this analysis, we have used the data exactly as reported in Planck Collaboration (2011a), that is, we use their redshifts, and we assume $h = 0.70$, though we note that the h value impact the amplitude a only at the 1% level. The only exception is cluster A2034, for which the redshift in Planck Collaboration (2011a) is clearly incorrect (Planck Collaboration 2011a, quote $z = 0.151$, while we use the cD galaxy redshift, $z = 0.113$, a very significant difference). These results are illustrated with the blue lines in Figure 3. Our best fit amplitude is in agreement with that quoted in Planck Collaboration (2011a), though our best fit value for the intrinsic scatter is lower, with $\Delta\sigma_{sz|x} \approx 0.04$ (partly because we have correct the redshift of cluster A2034), and our best fit slopes are flatter. Despite the differences noted above, we can conclude that the fitting method is not responsible for the difference between our results and those of Planck Collaboration (2011a).

We test the importance of using a subsample of Planck Collaboration (2011a) data by analyzing the Planck Collaboration (2011a) data, but restricting our analysis to the clusters employed in our *Chandra* analysis. In this case, we find $a = -0.166 \pm 0.035$, $\alpha = 0.912 \pm 0.043$, and $\sigma_{sz|x} = 0.132 \pm 0.036$. We see that the sample selection plays a significant impact on the results of the recovered Y_{SZ}/Y_X ratio for the *XMM* data. The higher normalization of the $Y_X - Y_{SZ}$ relation from the full *Planck* sample must therefore be driven by the remaining 34 clusters not in the *Chandra* subsample (most of which are at $z > 0.1$). Note that while we have not attempted to replicate the Monte Carlo analysis of Planck Collaboration (2011a) to try to estimate selection effects, their own tests suggest that there are negligible, having no impact on the amplitude of the Y_{SZ}–Y_X relation, and impacting the slope only at the $\Delta\alpha = 0.01$ level, much less than the statistical uncertainty in the measurement.

Even when restricting ourselves to the same galaxy clusters, however, the *Chandra* data results in a lower Y_{SZ}/Y_X ratio. While this difference is $< 1\sigma$ in terms of the statistical error bar, we note the statistical significance is significantly higher because both data sets share the same Y_{SZ} data, and it is the Y_{SZ} error that dominates the error budget. More specifically, the fact that both clusters use the exact same Y_{SZ} data implies that the the difference must be driven entirely by systematic differences in Y_X between the two data sets.

Aside from the differences in amplitude, it is interesting to note the difference in the intrinsic scatter estimate between the two data sets. The simplest interpretation of this result is that there are unidentified sources of stochasticity in the Planck Collaboration (2011a) X-ray analysis that result in an overestimate of the intrinsic scatter of the Y_{SZ}–Y_X relation of galaxy clusters.

Finally, it is worth noting that all of our fits consistently return a slope $\alpha \approx 0.91$, compared to the $\alpha = 0.96$ slope reported in Planck Collaboration (2011a). This difference appears to be due to the choice of fitting method: fitting our data using the same BCES method employed by Planck Collaboration (2011a), we recover $\alpha = 0.96$. Since we find no evidence for non-gaussian scatter intrinsic scatter in the $Y_{SZ} - Y_X$ relation, and furthermore, the observed scatter is dominated by measurement uncertainties, we believe that using the maximum likelihood fit is better justified.

The final data set that we compare against is that of Andersson et al. (2010), who find $\ln Y_{SZ}/Y_X = -0.20 \pm 0.1$ using *Chandra* X-ray data and SPT SZ data with a median cluster redshift $z \approx 0.7$. This value is essentially in perfect agreement with ours, and is also consistent

---

[7] The number quoted in Planck Collaboration (2011a) is 0.10 ± 0.010, but they quote scatter in dex, while we quote the scatter in $\ln Y_{SZ}$.

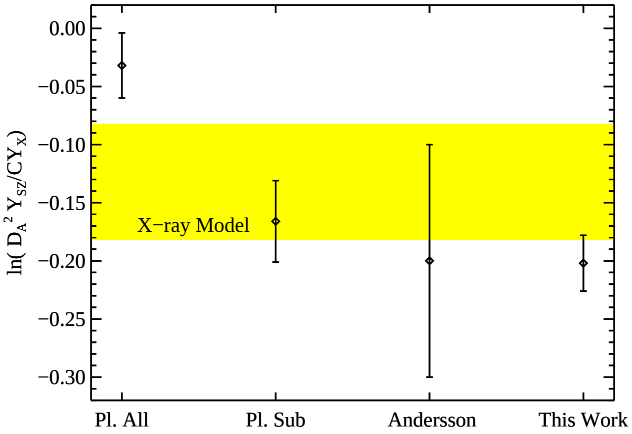

FIG. 5.— The Y_{SZ}/Y_X ratio, as observed using a variety of data. The horizontal band is our X-ray predictions model from section 2, the width of which (±0.05) reflect our ignorance of clumping corrections. The "Pl. All" data point shows our re-analysis of the Planck Collaboration (2011a) data. "Pl. Sub" uses this same data, but restricts the cluster sample to that employed in our *Chandra* analysis. The Andersson point comes from Andersson et al. (2010).

with that of Planck Collaboration (2011a). The uncertainty in their measurement is significantly larger than the one reported here or in Planck Collaboration (2011a) both because of a smaller cluster sample, and because the X-ray data is also shallower in terms of number of X-ray photons. We conclude that from the comparison of *Planck*+*Chandra* and SPT+*Chandra* samples, there is no evidence for evolution in the $Y_{SZ} - Y_X$ relation. It will be interesting to make the same comparison in the future as both projects acquire more galaxy clusters with high quality SZ and X-ray data.

For completeness, we have also estimated the amplitude of the Y_{SZ}–Y_X relation setting $\alpha = 1$ for both our data, and the various sub-samples of the Planck Collaboration (2011a) data we considered here. The likelihood for each of these fits is shown in Figure 6. In addition, we also computed the best fit amplitude for the low redshift ($z \leq 0.12$) and intermediate redshift ($0.12 < z < 0.3$) sub-samples from Planck Collaboration (2011a). Our results are summarized in Figure 5.

6.2. *Comparison to X-ray Expectations*

Our empirical calibration of the $Y_{SZ} - Y_X$ relation for $z < 0.1$ Planck clusters is somewhat lower than the expectation from the observed cluster temperature profiles for both *Chandra* and *XMM* measurements, $\Delta\ln(Y_{SZ}/Y_X)_{XMM} = -0.09 \pm 0.035$ and $\Delta\ln(Y_{SZ}/Y_X)_{Chandra} = -0.127 \pm 0.024$. Some of this offset can be explained by small-level nonuniformities of the intracluster gas (gas clumping factor Q in eq. 8). As per our earlier discussion, we set $Q = 1.05 \pm 0.05$ (Nagai et al. 2007), which brings the predicted Y_{SZ}/Y_X ratio within a few percent of the observed value, $\Delta\ln(Y_{SZ}/Y_X)_{XMM} = 0.09$ for the full *XMM*–*Planck* cluster sample, $\Delta\ln(Y_{SZ}/Y_X)_{XMM} = -0.042 \pm 0.035$ for the *Chandra* sub-sample of galaxy clusters, and $\Delta\ln(Y_{SZ}/Y_X)_{Chandra} = -0.078 \pm 0.024$ as estimated from *Chandra*. Note that the estimated systematic uncertainty in the clumping correction is ±0.05, so all values are in reasonable agreement with expectations, even though some are in strong statistical tension with one another.

Our results fit within the general picture that has developed in the recent past. A few years back, a variety of works argued that the SZ signal of galaxy clusters was inconsistent with predictions from X-ray data (Lieu et al. 2006; Bielby & Shanks 2007). These authors fit isothermal β models to *ROSAT* data in order to predict the SZ-signal of galaxy clusters as observed by WMAP, finding that the observed SZ signal was significantly lower than that their predictions. There is now ample evidence that β models are inadequate fits to the intra-cluster gas of galaxy clusters (e.g Vikhlinin et al. 2006; Croston et al. 2008), and that clusters are not isothermal (e.g. Vikhlinin et al. 2006; Pratt et al. 2007; Sun et al. 2009; Moretti et al. 2011). Hallman et al. (2007) and Mroczkowski et al. (2009) explicitly demonstrated that isothermal model fits to X-ray data leads one to over-predict the SZ signal of galaxy clusters. Using more realistic density and temperature profiles, one finds good agreement between SZ and X-ray observables (Atrio-Barandela et al. 2008; Komatsu et al. 2008; Mroczkowski et al. 2009; Diego & Partridge 2010; Zwart et al. 2011; Melin et al. 2011; Planck Collaboration 2011a,c). The results summarize above fit well within this new wave of works.

7. SUMMARY AND CONCLUSIONS

Using SZ data from *Planck* (Planck Collaboration 2011a) and X-ray data from *Chandra* (Vikhlinin et al. 2009), we have estimated the Y_{SZ}–Y_X scaling relation. Assuming a power-law of the form in equation 12, we find $\ln(Y_{SZ}/Y_X) = a = -0.202 \pm 0.024$, $\alpha = 0.916 \pm 0.032$, and $\sigma_{sz|x} = 0.083 \pm 0.021$. The scatter constraint is prior-driven, and the variance in the relation is consistent with zero intrinsic scatter. The slope α differs from unity at the $\approx 2.3\sigma$ level, which is interesting but not yet significant. We find no significant difference in the scaling relations when comparing relaxed and unrelaxed systems.

Our mean Y_{SZ}/Y_X is significantly lower than that reported from the *XMM* and *Planck* analysis of the full sample of 62 clusters ($a = -0.032 \pm 0.028$). However, when we repeat the *Planck* and *XMM* analysis restricting ourselves to the same 28 systems that compose the *Chandra* subsample, we find results that are in significantly better agreement ($a = -0.166 \pm 0.036$), demonstrating the original tension is driven by the remaining 34 (mostly $z \geq 0.1$) clusters in the full *Planck* and *XMM* cluster sample.

Compared with the *XMM-Newton* analysis, we find a significantly lower scatter in the $Y_{SZ} - Y_X$ relation, $\sigma_{sz|x} = 0.083 \pm 0.021$ for the *Chandra*–*Planck* data, versus $\sigma_{sz|x} = 0.182 \pm 0.025$ for the full *XMM*–*Planck* sample. The scatter for the full *XMM*–*Planck* sample is at least partly driven by the systematic differences between the *Chandra* sub-sample of galaxy clusters, and the remaining systems. The *XMM*–*Planck* scatter for the *Chandra* subsample is lower $\sigma_{sz|x} = 0.132 \pm 0.036$ and consistent with the scatter estimated from *Chandra* data. Finally, we note the *Chandra* data is fully consistent with no intrinsic scatter in the Y_{SZ}–Y_X relation: our central values are prior-driven.

Both the *Chandra* and *XMM* values of Y_{SZ}/Y_X for $z < 0.1$ are significantly lower than $a = -0.075$ expected from the observed cluster temperature profiles along (§ 2). We believe that a significant fraction of that difference can be attributed to some level of gas clumping, with $Q \simeq 1.05$ including substructure masking (Nagai et al. 2007). Any remaning difference is within the range of current absolute accuracy of the X-ray temperature measurements and systematic uncertainty in the clumping factor correction.

In summary, we find that the observed $Y_X - Y_{SZ}$ relation from the joint *Planck* and *Chandra* analysis is in good agreement with the theoretical expectations — it shows very low intrinsic scatter, a slope close to unity, and the amplitude is consistent with physically plausible levels of gas clumping.

In conjunction with the work in Vikhlinin et al. (2009), our results can be used to self-consistently estimate the multi-variate scaling relation of galaxy clusters. In an upcoming work, we use these results to study the L_X–M and Y_{SZ}–M scaling relations of galaxy clusters as determined from X-ray data, and compare these to those derived from the optically selected maxBCG galaxy cluster catalog (Koester et al. 2007).

The authors would like to thank August Evrard, James Bartlett, and Eli Rykoff for useful discussions, and comments on draft versions of the manuscript. We also thank Monique Arnaud and Gabriel Pratt for useful criticism on an earlier draft of this work. ER is funded by NASA through the Einstein Fellowship Program, grant PF9-00068. AV is funded by NASA grant GO1-12168X and contract NAS8-39073. SM is supported by the KICP through the NSF grant PHY-0551142 and an endowment from the Kavli Foundation.

REFERENCES

Allen, S. W. et al. 2008, MNRAS, 383, 879
Andersson, K. et al. 2010, ArXiv e-prints: 1006.3068
Arnaud, M., Pointecouteau, E., & Pratt, G. W. 2007, A&A, 474, L37
Arnaud, M. et al. 2010, A&A, 517, A92+
Atrio-Barandela, F. et al. 2008, ApJ, 675, L57
Becker, M. R. & Kravtsov, A. V. 2010, ArXiv e-prints: 1011.1681
Benson, B. A. et al. 2011, ArXiv e-prints
Bielby, R. M. & Shanks, T. 2007, MNRAS, 382, 1196
Bonamente, M. et al. 2008, ApJ, 675, 106
Carlstrom, J. E. et al. 2011, PASP, 123, 568
Cavagnolo, K. W. et al. 2009, ApJS, 182, 12
Comis, B. et al. 2011, MNRAS, 418, 1089
Croston, J. H. et al. 2008, A&A, 487, 431
Diego, J. M. & Partridge, B. 2010, MNRAS, 402, 1179
Evrard, A. E. et al. 2008, ApJ, 672, 122
Fabjan, D. et al. 2011, ArXiv e-prints
Foley, R. J. et al. 2011, ApJ, 731, 86
Fowler, J. W. et al. 2007, Appl. Opt., 46, 3444
Gull, S. F. & Northover, K. J. E. 1976, Nature, 263, 572
Hallman, E. J. et al. 2007, ApJ, 665, 911
Holder, G., Haiman, Z., & Mohr, J. J. 2001, ApJ, 560, L111
Jeltema, T. E. et al. 2008, ApJ, 681, 167
Kay, S. T. et al. 2011, ArXiv e-prints
Koester, B. et al. 2007, ApJ, 660, 239
Komatsu, E. et al. 2008, ArXiv e-prints, 803
Kravtsov, A. V., Vikhlinin, A., & Nagai, D. 2006, ApJ, 650, 128
Lau, E. T., Kravtsov, A. V., & Nagai, D. 2009, ApJ, 705, 1129
Lieu, R., Mittaz, J. P. D., & Zhang, S.-N. 2006, ApJ, 648, 176
Mantz, A. et al. 2010, MNRAS, 406, 1773
Marriage, T. A. et al. 2011, ApJ, 737, 61
Mathiesen, B., Evrard, A. E., & Mohr, J. J. 1999, ApJ, 520, L21
Melin, J.-B. et al. 2011, A&A, 525, A139+
Menanteau, F. et al. 2011, ArXiv e-prints: 1109.0953
Meneghetti, M. et al. 2010, A&A, 514, A93+
Moretti, A. et al. 2011, A&A, 528, A102
Mroczkowski, T. et al. 2009, ApJ, 694, 1034
Nagai, D. 2006, ApJ, 650, 538
Nagai, D., Vikhlinin, A., & Kravtsov, A. V. 2007, ApJ, 655, 98
Piffaretti, R. & Valdarnini, R. 2008, A&A, 491, 71
Planck Collaboration. 2011a, ArXiv e-prints: 1101.2026
—. 2011b, ArXiv e-prints: 1101.2025
—. 2011c, ArXiv e-prints: 1101.2043
—. 2011d, ArXiv e-prints: 1101.2024
—. 2011e, ArXiv e-prints: 1101.2022
—. 2011f, ArXiv e-prints
Pratt, G. W. et al. 2007, A&A, 461, 71
—. 2009, A&A, 498, 361
Rasia, E. et al. 2012, ArXiv e-prints
Rozo, E. et al. 2011, In preparation
Sehgal, N. et al. 2011, ApJ, 732, 44
Sifon, C. et al. 2012, ArXiv e-prints
Stanek, R. et al. 2010, ApJ, 715, 1508
Sun, M. et al. 2009, ApJ, 693, 1142
Sunyaev, R. A. & Zeldovich, Y. B. 1972, Comments on Astrophysics and Space Physics, 4, 173
Vanderlinde, K. et al. 2010, ApJ, 722, 1180
Vikhlinin, A. et al. 2005, ApJ, 628, 655
—. 2006, ApJ, 640, 691
—. 2009, ApJ, 692, 1033
Zwart, J. T. L. et al. 2011, MNRAS, 418, 2754

APPENDIX

CLUSTER DATA

We summarize the data employed in our analysis in table 1.

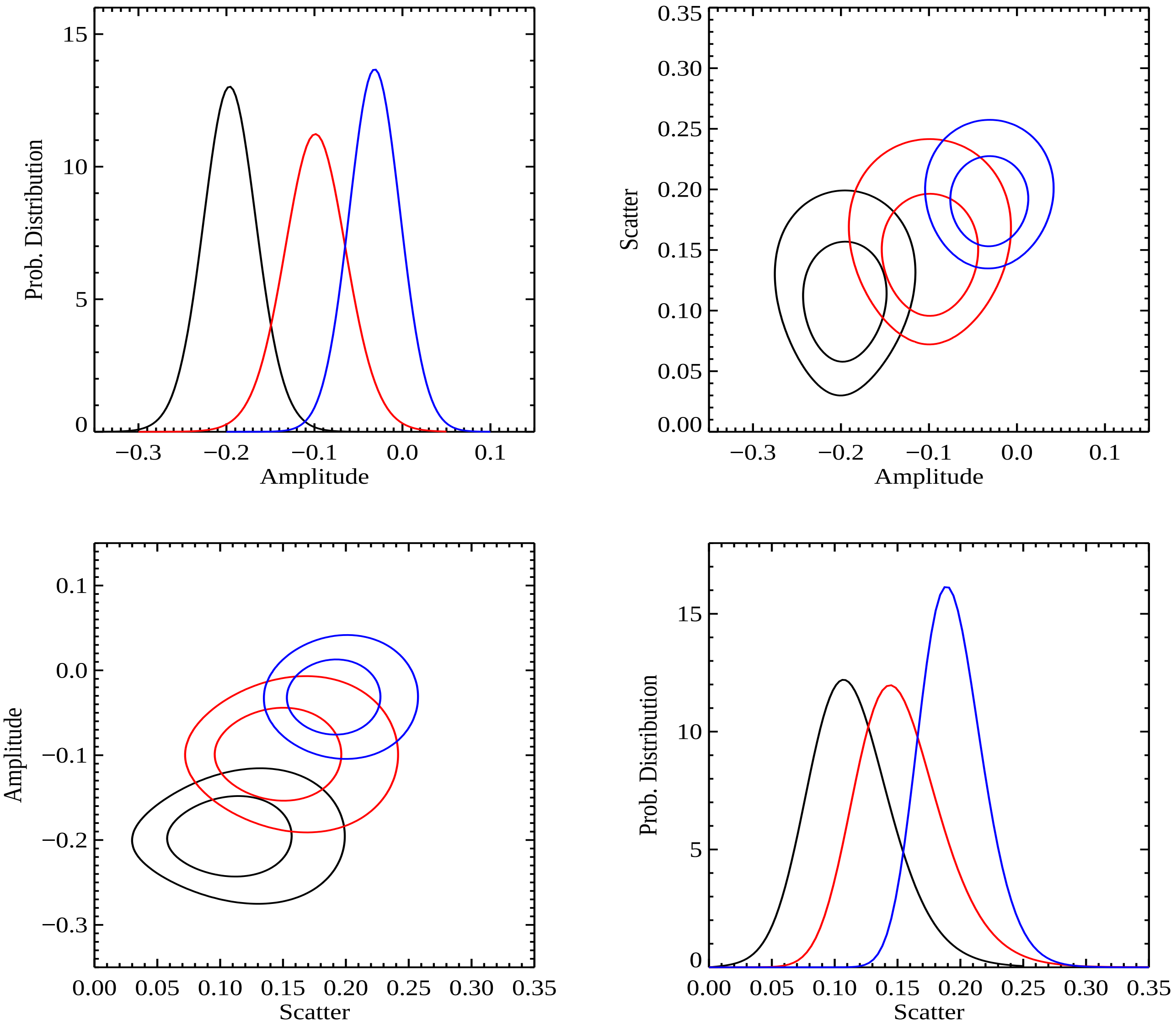

Fig. 6.— Best-fit parameters for the Y_{SZ}–Y_X scaling relation assuming a slope of unity. Black curves are obtained using *Chandra* data and the cluster sample in Table 1. Red and blue curves are using the Planck Collaboration (2011a) data. The red curves show the results when we restrict our analysis of the Planck Collaboration (2011a) data to the same galaxy clusters that constitute our *Chandra* sample. The blue curves include all galaxy clusters in Planck Collaboration (2011a). All confidence regions are 68% and 95% likelihood contours respectively.

TABLE 1
Cluster Data

Name	P11 Redshift	Redshift	$D_A^2 Y_{SZ}$	CY_X (*Chandra*)	CY_X (*XMM*)	Merger?
A85	0.052	0.0557	5.05 ± 0.54	6.19 ± 0.16	5.37 ± 0.22	—
A119	0.044	0.0445	2.60 ± 0.29	3.55 ± 0.13	3.42 ± 0.16	✓
A401	0.075	0.0743	7.71 ± 0.74	10.86 ± 0.47	10.42 ± 0.75	—
A3112	0.070	0.0759	1.98 ± 0.33	3.38 ± 0.21	2.82 ± 0.11	—
A3158	0.060	0.0583	3.14 ± 0.27	3.10 ± 0.07	3.73 ± 0.15	—
A478	0.088	0.0881	8.71 ± 0.76	10.17 ± 0.58	9.59 ± 0.39	—
A3266	0.059	0.0602	8.84 ± 0.69	11.89 ± 0.29	10.07 ± 0.36	✓
A3376	0.045	0.0455	0.97 ± 0.19	1.64 ± 0.24	1.34 ± 0.06	✓
A1413	0.143	0.1429	6.99 ± 0.76	7.83 ± 0.48	7.58 ± 0.12	—
ZwCl1215	0.077	0.0767	4.32 ± 0.66	5.54 ± 0.21	5.72 ± 0.30	—
A3528s	0.053	0.0574	2.41 ± 0.33	2.00 ± 0.15	1.62 ± 0.10	—
A1644	0.047	0.0475	2.41 ± 0.39	3.08 ± 0.30	2.80 ± 0.13	✓
A1650	0.084	0.0823	4.00 ± 0.55	3.62 ± 0.15	3.67 ± 0.08	—
A1651	0.084	0.0853	3.50 ± 0.58	5.32 ± 0.29	4.12 ± 0.12	—
A1689	0.183	0.1828	12.93 ± 1.42	13.42 ± 0.71	12.41 ± 0.22	—
A3558	0.047	0.0469	3.95 ± 0.47	4.04 ± 0.36	4.50 ± 0.18	✓
A1795	0.062	0.0622	4.37 ± 0.38	5.34 ± 0.18	6.78 ± 0.28	—
A1914	0.171	0.1712	9.47 ± 0.85	13.29 ± 0.68	12.43 ± 0.31	—
A2034	0.151	0.1130	4.27 ± 0.58	5.11 ± 0.15	6.01 ± 0.14	—
A2029	0.078	0.0779	7.65 ± 0.66	11.48 ± 0.53	12.13 ± 0.65	—
A2065	0.072	0.0723	3.72 ± 0.48	4.35 ± 0.16	4.52 ± 0.23	✓
A2163	0.203	0.2030	43.01 ± 1.99	60.93 ± 3.21	59.75 ± 2.14	✓
A2204	0.152	0.1511	10.39 ± 0.94	12.96 ± 1.00	11.88 ± 0.39	—
A2256	0.058	0.0581	6.73 ± 0.38	8.94 ± 0.43	7.02 ± 0.33	✓
A2255	0.081	0.0800	4.81 ± 0.37	4.97 ± 0.14	4.81 ± 0.15	—
RX J1720	0.164	0.1593	5.68 ± 0.72	6.45 ± 0.38	5.69 ± 0.14	—
A2390	0.231	0.2302	15.61 ± 1.22	19.49 ± 1.56	19.26 ± 0.58	—
A3921	0.094	0.0941	3.41 ± 0.28	3.75 ± 0.15	3.10 ± 0.08	—

Note. — The units for $D_A^2 Y_{SZ}$ and CY_X are 10^{-5} Mpc^2. The Y_X values from *XMM* are drawn from Planck Collaboration (2011a). In addition, both the Y_{SZ} and Y_X data of Planck Collaboration (2011a) are corrected to our fiducial cosmology ($h = 0.72$) and to our cluster redshifts. The P11 redshift column quotes the redshifts as they appear in Planck Collaboration (2011a).